

ORIGINAL PAPERS

Homotypic and heterotypic interactions of EWS, FLI1 and their oncogenic fusion protein

Laura Spahn^{1,3}, Christine Siligan^{1,3}, Radostina Bachmaier¹, Johannes A Schmid², Dave NT Aryee¹ and Heinrich Kovar^{*,1}

¹Children's Cancer Research Institute, St Anna Kinderspital, A-1090 Vienna, Austria; ²Department of Vascular Biology and Thrombosis Research, University of Vienna, and Competence Center 'Bio-Molecular Therapeutics', 1235 Vienna, Austria

In Ewing's sarcoma family tumors, the ets transcription factor gene *FLI1* is rearranged with one *EWS* allele resulting in coexpression of germline *EWS* and chimeric *EWS-FLI1* proteins. Here, we investigated the potential of germline *EWS*, *FLI1* and *EWS-FLI1* to oligomerize. In two functional *in vivo* tests, fluorescence resonance energy transfer (FRET) and the mammalian two-hybrid (MTH) assay, self-association of *EWS* and *EWS-FLI1*, but not of *FLI1* was detected. In addition, interaction of *EWS-FLI1* with *EWS* and *FLI1* was observed. GST pull-down assays and immunoprecipitation experiments largely confirmed these results. The *EWS* N-terminal domain present in both *EWS* and *EWS-FLI1* was found to contribute to homotypic and heterotypic interactions of these proteins. However, in the context of germline *EWS*, the presence of the whole or part of the C-terminal RNA-binding domain greatly supported the self-association potential of the protein. Involvement of an RNA component in *EWS* oligomerization was confirmed by sensitivity of the corresponding GST pull-down assay to RNaseA treatment. In contrast, *EWS-FLI1* was able to self-associate and also bind to *FLI1* via its C-terminal domain, which comprises the *FLI1* DNA-binding motif. Accordingly, the *EWS-FLI1* interaction was not disrupted by RNaseA treatment. Despite its potential to oligomerize, *EWS-FLI1* bound to a tandem ets-binding site of the TGF β type II receptor promoter as a monomer. Therefore, the functional consequences of homo- and hetero-oligomerization of *EWS* and *EWS-FLI1* proteins remain to be elucidated.

Oncogene (2003) 22, 6819–6829. doi:10.1038/sj.onc.1206810

Keywords: *EWS*; *FLI1*; Ewing's sarcoma; dimerization; protein interaction

Introduction

Expression of the fusion protein *EWS-FLI1* is characteristic of Ewing's sarcoma family tumors (EFT), a

group of childhood neoplasia affecting bone and soft tissue. The protein is encoded by the fusion gene *EWS-FLI1*, which results from the chromosomal translocation t(11;22)(q24;q12) (Delattre *et al.*, 1992). The *EWS-FLI1* chimeric protein combines the N-terminal domain (NTD) of the putative RNA-binding protein *EWS* with the DNA-binding domain of the ets transcription factor *FLI1*, resulting in a unique protein with features of a transcription factor. *EWS-FLI1* binds to DNA in a sequence-specific manner and is able to activate transcription in reporter gene assays (Delattre *et al.*, 1992; May *et al.*, 1993; Ohno *et al.*, 1993; Bailly *et al.*, 1994). The replacement of the *FLI1* N-terminus by the *EWS* NTD, which is primarily composed of 31 repeats of a degenerate hexapeptide motif with the consensus SYGQQS, results in increased activity of *FLI1*-responsive reporter genes. Thus, the *EWS* NTD^{*EWS*} is considered a novel type of tyrosine-dependent transactivation domain (Feng and Lee, 2001). In addition, *EWS-FLI1* possesses transforming activity, which is not shared by the germline counterparts *EWS* and *FLI1* (May *et al.*, 1993). However, for full *in vitro* transforming activity, both domains, the *FLI1* carboxy terminus and the *EWS* amino terminus, are required (Lessnick *et al.*, 1995). The transformation capacity and the fact that sustained expression of *EWS-FLI1* is necessary for continued growth of EFT cells (Ouchida *et al.*, 1995; Kovar *et al.*, 1996; Toretsky *et al.*, 1997) indicates that *EWS-FLI1* plays a key role in EFT pathogenesis. Based upon its action as a transcription factor, it is reasonable to think that *EWS-FLI1* may deregulate expression or alter selection of *FLI1* target genes. Several putative *EWS-FLI1* regulated genes have been identified mostly in heterologous systems, only few of which might have transforming potential by themselves (Kovar *et al.*, 1996; Thompson *et al.*, 1996; May *et al.*, 1997; Arvand *et al.*, 1998; Hahm *et al.*, 1999; Dauphinot *et al.*, 2001; Matsumoto *et al.*, 2001; Zwerner and May, 2001; Lessnick *et al.*, 2002; Fukuma *et al.*, 2003). Results obtained with an *EWS-FLI1* mutant lacking a functional ets DNA-binding domain suggest that *EWS-FLI1* may have additional, transcription-independent functions in the cellular transformation process (Jaishankar *et al.*, 1999; Welford *et al.*, 2001). Protein interactions with several components of the RNA processing apparatus suggest that *EWS* and

*Correspondence: H Kovar; E-mail: heinrich.kovar@ccri.univie.ac.at

³These authors contributed equally

Received 26 March 2003; revised 8 May 2003; accepted 15 May 2003

EWS-FLI1 may play a role in the post-transcriptional regulation of gene expression. EWS-FLI1 associates with the spliceosome assembly factors SF1 and U1C (Zhang *et al.*, 1998; Knoop and Baker, 2000), interactions potentially altering 5' splice site selection (Knoop and Baker, 2001). However in contrast to EWS, EWS-FLI1 is unable to recruit YB1 and serine-arginine splicing proteins and may therefore uncouple transcription and splicing (Yang *et al.*, 2000; Chansky *et al.*, 2001). We recently reported the interaction between EWS and EWS-FLI1 with BARD1, the BRCA1-associated ring domain protein (Spahn *et al.*, 2002) possibly providing a link to mRNA polyadenylation, since BARD1 inhibits the function of CstF50, a subunit of the polyadenylation cleavage factor (Kleiman and Manley, 1999, 2001). In addition, BARD1 may be the bridging factor between EWS-FLI1 and BRCA1, an established tumor suppressor protein with multiple functions in transcription and DNA double-strand break repair (Venkitaraman, 2001).

Here, we report the homotypic and heterotypic interactions of EWS, FLI1 and EWS-FLI1 and the protein domains involved.

Results

Homotypic and heterotypic interactions of EWS, FLI1 and EWS-FLI1

During our studies on protein interactions of the EFT-associated chimeric oncogene EWS-FLI1 and its normal counterpart EWS using fluorescence resonance energy transfer (FRET) microscopy (Spahn *et al.*, 2002), we also observed homotypic associations of these proteins. FRET microscopy can visualize interaction of proteins *in vivo*, based upon energy transfer between two fluorophores (CFP and YFP) with overlapping emission/excitation spectra that are covalently attached to the interaction partners. Homotypic associations of EWS and EWS-FLI1 were monitored by donor recovery after acceptor photobleaching FRET microscopy. For this assay, a CFP picture is taken with the CFP filter and the same microscope and camera settings before and after photobleaching. Before bleaching, energy will be transferred from the CFP donor to the YFP acceptor if they come into close proximity, which results in quenching of CFP fluorescence. Photobleaching to destroy the YFP fluorophore was accomplished with full light through the YFP filter prohibiting energy transfer between CFP and YFP fluorophores and consequently resulting in the recovery of full CFP light emission. In the case of an interaction between the fluorophore-tagged proteins, the CFP image after bleaching should therefore be brighter than the image before bleaching, detectable as a positive $\text{CFP}_{\text{post}}/\text{CFP}_{\text{pre}}$ ratio image. As long as the YFP acceptor is expressed at similar or lower levels than the CFP donor, the method is independent of the absolute expression levels and cellular localization of the proteins of interest (Schmid *et al.*, 2001). As a positive control, the tandem

fusion CYFP (Schmid *et al.*, 2001) was used. For negative control, CFP, YFP and CFP- or YFP-EWS-FLI1 and CFP- or YFP-EWS were expressed separately (not shown). As shown in Figure 1a, positive ratio images were obtained when CFP- and YFP-tagged EWS and EWS-FLI1 proteins were coexpressed, suggesting that EWS and EWS-FLI1 are able to form homo-oligomers in the nucleus.

Since the donor recovery method monitors only the acceptor-dependent decrease in donor fluorescence and therefore frequently results in only faint positive ratio images (Figure 1a), the three-filter method was applied in all subsequent FRET experiments (Xia and Liu, 2001). Here, CFP, YFP and FRET filter images are used to calculate a normalized FRET image (FRET_N), which corrects for CFP and YFP bleed-through into the FRET channel. Based on these corrections, this method is completely independent of the expression levels of the tagged proteins (Schmid and Sitte, 2003). In contrast to the donor recovery method, which monitors only one part of the FRET effect (the acceptor-dependent reduction in donor fluorescence), the three-filter method monitors both the donor decrease and the acceptor increase due to FRET and thus results in a higher net-signal and a better signal-to-noise ratio. However, the three-filter method requires external controls for the calculation of correction factors, while the donor recovery technique provides an internal control. Otherwise, both methods are qualitatively equal.

Using the three-filter method, we determined the self-association properties of germline FLI1 which has previously been demonstrated to interact with other ets proteins, including ERG and TEL, via its N-terminal pointed domain (Mavrothalassitis and Ghysdael, 2000), and of the isolated EWS NTD^{EWS} present in EWS and EWS-ets fusion proteins. While a clear self-association of NTD^{EWS} was noted, we could not detect an interaction of tagged FLI1 with itself as demonstrated by the lack of a positive FRET_N image (Figure 1b).

In order to confirm the FRET results and to also test heterotypic interactions between EWS and/or FLI1 with EWS-FLI1, we employed the mammalian two-hybrid (MTH) system. Two-hybrid systems are based on the reconstitution of a functional transcription factor from a DNA-binding domain and a transactivation domain via the interaction of two hybrid proteins. As depicted in Figure 2a, we generated fusions of all three full-length and several truncated EWS and FLI1 proteins with the GAL4-DNA-binding domain, as well as with the VP16 transactivation domain and tested them in SJ-NB7 cells for activation of transcription from a luciferase reporter construct. The results (presented as fold increase in luciferase activity relative to the activity of the GAL4-DBD fusion alone, Figure 2b) largely confirm the observations from the *in vivo* FRET microscopy experiments. As expected, GAL4-EWS-FLI1 already activated luciferase expression due to the presence of the N-terminal EWS domain, which serves as a potent transactivation domain in the context of EWS-FLI1 (May *et al.*, 1993) (not shown). However, coexpression of GAL4-EWS-FLI1 with VP16-EWS-FLI1 resulted in

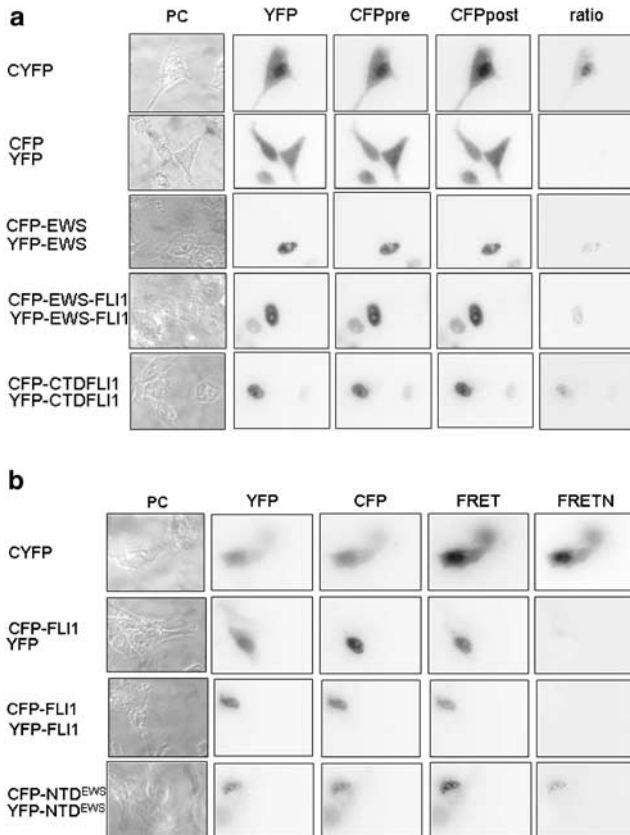


Figure 1 FRET analysis of homotypic interactions of EWS, EWS-FLI1, FLI1 and their subdomains. **(a)** Homo-oligomerization of EWS, EWS-FLI1 and CTD^{FLI1}, analysed by acceptor photobleaching FRET microscopy. Images show localization of CYFP, CFP and YFP in the cytoplasm and the nucleus, whereas the fusion proteins of EWS, EWS-FLI1 and CTD^{FLI1} were located exclusively in the nucleus. PC: phase contrast image; YFP, CFP_{pre}: respective filter images before bleaching; CFP_{post}: CFP-filter image after bleaching of the YFP acceptor; ratio: calculated ratio of the images CFP_{post}/CFP_{pre}. The filter images were acquired with identical microscope and camera settings. The interaction between two fluorophore-tagged proteins results in a weak ratio image restricted to the compartment where the interaction took place. In the absence of an interaction, the ratio image is blank, as in the case of cotransfected, uncoupled CFP and YFP proteins (negative control). Similarly, blank ratio images were obtained when the CFP- and YFP-fusion constructs were transfected separately (not shown). Positive FRET images were obtained for the positive control CYFP, and for coexpression of CFP-EWS/YFP-EWS, CFP-EWS-FLI1/YFP-EWS-FLI1 and CFP-CTD^{FLI1}/YFP-CTD^{FLI1} in nine of 12, six of six and 18 of 18 cotransfected cells, respectively. **(b)** Homo-oligomerization of FLI1, and NTD^{EWS} analysed by three-filter FRET microscopy. YFP, CFP and FRET represent images taken with the respective filters under identical conditions. The FRET_N image was generated by subtracting the bleed-through of YFP and CFP fluorescence into the FRET filter image and therefore represents the fluorescence due to FRET only. The correction factors for the bleed-through were determined using cells expressing CFP or YFP only (data not shown). In case of an interaction, the signal obtained with the FRET filter set (donor excitation, acceptor emission) persists after correction for bleed-through, whereas it is erased without interaction of donor and acceptor proteins. As a negative control, the result for the cotransfection of CFP-FLI1/YFP is shown. Similar negative results were obtained for the reciprocal combinations CFP/YFP-FLI1, CFP-NTD^{EWS}/YFP, CFP/YFP-NTD^{EWS} and CFP/YFP only (not shown). Positive FRET_N images were obtained for the positive control CYFP and for CFP-NTD^{EWS}/YFP-NTD^{EWS} (seven of 12 cotransfected cells), but not for the CFP-FLI1/YFP-FLI1 combination (12 of 13 cotransfected cells negative, one ambiguous)

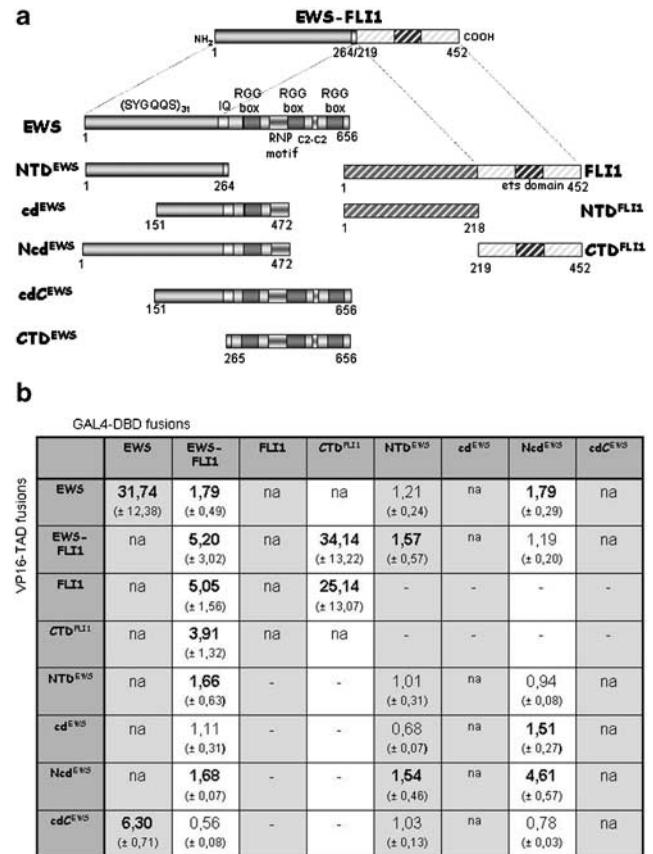


Figure 2 MTH analysis. **(a)** Schematic representation of the MTH constructs. Construct names, as used in the text with the protein assignments in superscript: NTD, N-terminal domain; cd, central domain; Ncd, N-terminal plus central domain; cdC, central plus C-terminal domain; CTD, C-terminal domain. Numbers below the constructs indicate flanking amino acid positions. (SYGQQS)₃₁: consensus sequence of hexapeptide repeats in the EWS amino terminus, IQ: IQ domain of EWS, RGG boxes and RNP motif: RNA-binding domain of EWS, C2-C2: Zn-finger-like domain, ets domain: conserved ets DNA-binding domain of FLI1. All proteins were tagged at their N-terminus with either the GAL4-DNA-binding domain or the VP16-transactivation domain, respectively. **(b)** Results of interaction analysis in the MTH system. Rows: VP16-transactivation domain fusions, columns: GAL4-DNA-binding domain fusions. Values represent the luciferase activity of the tested pairings relative to the activity of the respective GAL4-DBD fusion only. All transformations were carried out in triplicate and repeated five times on average. Individual results were corrected for transfection efficiency, which was determined by cotransfection of GFP. As positive and negative controls, reporter gene activation by GAL4-NTD^{EWS} and empty vectors was routinely determined in all experiments. The mean relative light units (RLU) obtained for GAL4-NTD^{EWS} plus empty pACT were 791 000, while the combination of empty vectors (pBIND + pACT) resulted in a background activity of 9200 units. Values of less than 0.06 times the value obtained for GAL4-NTD^{EWS} were considered as indicative of no activation (na). Transfection of VP16-TAD fusion constructs with empty pBIND vector resulted in background activity only. Transfection of GAL4-DBD fusions with empty pACT also resulted in background activity, except for GAL4-NTD^{EWS}, GAL4-EWS-FLI1 (0.38 times GAL4-NTD^{EWS}) and GAL4-Ncd^{EWS} (0.52 times GAL4-NTD^{EWS}). The numbers given are mean values of all performed measurements with standard deviations indicated in parentheses. Numbers in bold are judged positive for interaction and are referred to in the text. -: not determined

a 5.2-fold higher luciferase activity, indicating the formation of an EWS-FLI1 homo-oligomer. The GAL4-EWS and VP16-EWS constructs alone showed only background activity compatible with an earlier notion that the transactivation potential of the EWS N-terminus is repressed in cis by its C-terminus (Li and Lee, 2000) (not shown). Upon coexpression of the fusion proteins, reporter gene activity increased more than 30-fold over background, clearly demonstrating the self-association of EWS. Coexpression of GAL4-FLI1 and VP16-FLI1 did not result in any significant increase of reporter gene activity over the background, confirming the lack of interaction as already suggested by the FRET results.

EWS or FLI1 interaction with EWS-FLI1 in the MTH system depended on the type of two-hybrid constructs. VP16-EWS-FLI1 was not able to cooperate with GAL4-EWS or GAL4-FLI1, although all proteins were expressed at comparable levels (data not shown). It should be noted that not even GAL4-FLI1 alone was able to activate luciferase activity, despite carrying the genuine FLI1 transactivation domain. However, VP16-EWS and VP16-FLI1 enhanced GAL4-EWS-FLI1-mediated transactivation 1.8- and fivefold, respectively. The architecture-dependent discrepancies in transcriptional cooperation between VP16- and GAL4-fusion proteins may be due to different effects of these domains on the proper folding of the protein interaction surface. Thus, protein interaction between EWS-FLI1 and its germline counterpart EWS may be possible, but in comparison to the homotypic interactions, it seems to be weak and context-dependent. In order to exclude unspecific protein interactions of overexpressed EWS as the basis for cooperativity with EWS and EWS-FLI1, we combined GAL4- and VP16-tagged EWS and FLI1 in the MTH assay. Here, no interaction was observed irrespective of the constructs used. This result suggests that there is no affinity between EWS and FLI1 at all.

Self-association of EWS involves N-terminal and central residues

To determine the domains involved in homotypic and heterotypic interactions of EWS and EWS-FLI1, several deletion constructs (Figure 2a) were tested for interaction with each other and with the full-length proteins. First, we investigated the interaction properties of the EWS N-terminal domain (NTD^{EWS}; amino acids 1–264), which is shared by EWS and EWS-FLI1 and may therefore be involved both in the self-association of the two proteins and their interaction with each other. As already demonstrated in Figure 1b, the fluorophore-tagged NTD^{EWS} showed clear interaction with itself in the three-filter FRET method. Interestingly, in cells showing strong expression of the fusion proteins, the interaction took place in spot-like structures distributed throughout the nucleus, but excluding the nucleoli and cytoplasm (Figure 1b). However, this result could not be confirmed in the MTH system (Figure 2b). The expression of GAL4-NTD^{EWS} alone resulted in strong luciferase activity, consistent with the proposed function

of NTD^{EWS} as a potent transactivation domain in the EWS-FLI1 fusion protein (Lessnick *et al.*, 1995). In fact, transcriptional activation by GAL4-NTD^{EWS} was used as positive control throughout all MTH assays. Coexpression of GAL4-NTD^{EWS} with VP16-NTD^{EWS} did not further increase the level of reporter gene expression when compared to the activity of GAL4-NTD^{EWS} alone. The transcriptional activation properties of NTD^{EWS} have previously been demonstrated to be context-dependent and to be blocked by the presence of the EWS C-terminal domain (CTD) (Li and Lee, 2000). Thus, the inability of VP16-NTD^{EWS} to enhance transactivation in the MTH system may be due to structural constraints of the VP16 domain on the NTD^{EWS}. Likewise, coexpression of VP16-NTD^{EWS} with GAL4-EWS did not result in reporter gene activation, while there was a slight increase (about 1.7-fold) in luciferase activity when VP16-NTD^{EWS} was combined with GAL4-EWS-FLI1. Similarly, GAL4-NTD^{EWS} mediated transactivation was only marginally increased, about 1.6- and 1.2-fold, by VP16-EWS-FLI1 and VP16-EWS, respectively. Together, these data suggest that EWS amino acids 1–265 are not sufficient to mediate an effective and strong association with full-length EWS or EWS-FLI1, although they may contribute to the interaction surface in the overall protein context. Expansion of this domain to include the central domain (cd^{EWS}), which is disrupted by the gene fusion to an ets protein in the majority of EFT, in the construct Ncd^{EWS} (amino acids 1–472) partially rescued the cooperation with full-length EWS only if coupled to the GAL4 domain (1.8-fold increase in luciferase activity). When combined with GAL4-EWS-FLI1, VP16-Ncd^{EWS} increased reporter gene activity 1.7-fold, but no activity was observed when GAL4 and VP16 domains were exchanged for each other. Interestingly, the combination of VP16-Ncd^{EWS} with GAL4-Ncd^{EWS} led to a 4.6-fold increase in reporter gene transactivation. While VP16-NTD^{EWS} did not increase the activity of GAL4-Ncd^{EWS}, VP16-Ncd^{EWS} only marginally enforced reporter gene activity driven by GAL4-NTD^{EWS}. The isolated cd^{EWS} showed no interaction with any of the constructs. The only exception was the combination of VP16-cd^{EWS} with GAL4-Ncd^{EWS}, which showed a slight increase in reporter gene activity over GAL4-Ncd^{EWS} (1.5-fold). Since in a previous study (Bertolotti *et al.*, 1998) it has been mentioned that EWS would interact with its isolated CTD in GST pull-down experiments, we turned to the analysis of constructs containing EWS amino acids 265–656 (CTD^{EWS}) which are contained in germline EWS, but not EWS-FLI1. These constructs overlap with Ncd^{EWS} by 212 amino acids. However, the CTD^{EWS} showed neither interaction activity with itself, nor with full-length EWS in the MTH assay (not shown). Surprisingly, when fused to the VP16 domain, extension of the CTD^{EWS} to include the complete central domain (cd^{EWS}, amino acids 151–656) enhanced cooperation with GAL4-EWS 6.3-fold, while no interaction was observed between cd^{EWS} and EWS-FLI1, NTD^{EWS} and Ncd^{EWS}. These results may indicate a role for the RNA-binding domain in the homo-oligomerization of EWS.

However, since neither CTD^{EWS} (not shown) nor cdC^{EWS} containing the RNA-binding domain were able to oligomerize, an indirect interaction via RNA is highly unlikely. Overall, our results strongly suggest a strictly structure-dependent interaction mechanism of EWS that involves N-terminal and centrally localized amino acids. However, optimal association is only possible between full-length EWS molecules.

EWS-FLI1 interacts with itself via the FLI1 CTD

As the EWS NTD may not be sufficient to mediate self-association of EWS-FLI1, we generated MTH and FRET constructs of the FLI1 CTD^{FLI1} (germline FLI1 residues 219–452, corresponding to EWS-FLI1 type 1 amino acid residues 265–498). This domain contains the ets-DNA-binding domain of FLI1 and a putative C-terminal transactivation domain (Bertolotti *et al.*, 1998; Ohno *et al.*, 1993) but not the pointed domain, which is known to be involved in protein–protein interactions between different ets proteins (Li *et al.*, 2000). First, we tested the constructs GAL4-CTD^{FLI1} and VP16-CTD^{FLI1} separately and in combination with each other in the MTH system (Figure 2b). The isolated CTD^{FLI1} constructs were unable to drive reporter gene activation, not even when coupled to the GAL4-DNA-binding domain, despite a previous report demonstrating 40% of the full-length FLI1 transactivation capacity for CTD^{FLI1} (Rao *et al.*, 1993; Bertolotti *et al.*, 1998) (not shown). Likewise, coexpression of the CTD^{FLI1} constructs did not result in significant luciferase activity, although the fusion proteins were expressed in similar amounts (data not shown). This result would suggest that the CTD of FLI1 is not able to interact with itself. In contrast, with the FRET three-filter method, an association between CFP-CTD^{FLI1} and YFP-CTD^{FLI1} was clearly detectable (Figure 1a), indicating that the FLI1 C-terminus behaves differently in the context of the CFP- and YFP-chimera than in fusion with the GAL4-DNA-binding and the VP16-transactivation domain.

Next, we tested if CTD^{FLI1} is capable of interacting with EWS-FLI1 in the MTH system providing one CTD^{FLI1} in its genuine context. Coexpression of GAL4- or VP16-fused CTD^{FLI1} with the complementing EWS-FLI1 fusion constructs resulted in significantly enhanced reporter gene activation in the MTH system (34-fold when CTD^{FLI1} was provided as a GAL4 fusion and 3.9-fold, when GAL4-EWS-FLI1 was used as the DNA-binding two-hybrid component) (Figure 2b). These results suggest that the FLI1 C-terminus is significantly involved in the homo-oligomerization of EWS-FLI1. Likewise, combining full-length GAL4-EWS-FLI1 and VP16-FLI1 in the MTH assay revealed cooperation of these proteins to activate reporter gene activity fivefold. The reciprocal combination suggested a fourfold activation; however, absolute values were too low to consider them as significant. As expected, coexpression of full-length EWS and the CTD^{FLI1} did not result in reporter gene activation.

Although no homotypic interaction between full-length FLI1 proteins was observed, we further tested if

full-length FLI1 is capable of associating with its isolated C-terminus. In the combination of VP16-FLI1 with GAL4-CTD^{FLI1}, a remarkable increase (25-fold) in reporter gene activity was observed, while the *vice versa* combination did not result in measurable luciferase activity, although both proteins were expressed to similar extents (data not shown). Together, these results suggest that EWS-FLI1 is capable of interacting with itself and theoretically also with germline FLI1 through the FLI1 CTD, while FLI1 is unable to form homo-oligomers.

Confirmation of homotypic and heterotypic interactions of EWS and EWS-FLI1 by physical interaction assays

To confirm the interactions observed in the functional assays *in vitro*, GST pull-down assays and immunoprecipitations of recombinant proteins were performed (Figure 3). When incubated with purified GST, GST-EWS or GST-EWS-FLI1, both ³⁵S-labeled EWS and EWS-FLI1 were retained by GST-EWS and GST-EWS-FLI1, but not by GST alone. Firefly luciferase, which served as an unrelated control, did not bind to any of the GST proteins. Thus, the homotypic and heterotypic interactions of EWS and EWS-FLI1 in the pull-down experiment were considered as specific (Figure 3a). Since EWS is an RNA-binding protein, we tested if the observed interaction involved an RNA component. The GST pull-down assay was repeated in the absence and presence of RNaseA. As demonstrated in Figure 3b, RNaseA treatment reduced the ability of GST-EWS to retain *in vitro* translated EWS. Even after preincubation of the *in vitro* translated protein with RNaseA (not shown), the interaction was not completely wiped out indicating that an RNA component supports, but is not necessary for the homotypic association of EWS. In contrast, the interaction between EWS and GST-EWS-FLI1 was not affected by RNaseA treatment. These results suggest that the supramolecular structural requirements differ for homotypic and heterotypic interactions of EWS.

Finally, we tried to precipitate complexes of FLAG- and YFP-tagged EWS and EWS-FLI1 proteins from transfected SJ-NB7 cells using an anti-FLAG antibody. Precipitates were probed on the Western blot with an antiserum to the EWS N-terminus (139-2) (Figure 4). While it was possible to recover YFP-EWS-FLI1 with FLAG-EWS-FLI1 (Figure 4a) and with FLAG-EWS (Figure 4b), we were unable to obtain coimmunoprecipitates between differently tagged EWS proteins (not shown). This result may in part be due to low yield expression of YFP-tagged EWS in comparison to all other constructs. Generally, in repeated experiments, successful coimmunoprecipitations were much less reproducible than GST pull-down results.

Oligomerization is not involved in DNA binding of EWS-FLI1

EWS-FLI1 binds to DNA in a sequence-specific manner. The best-characterized direct target for EWS-

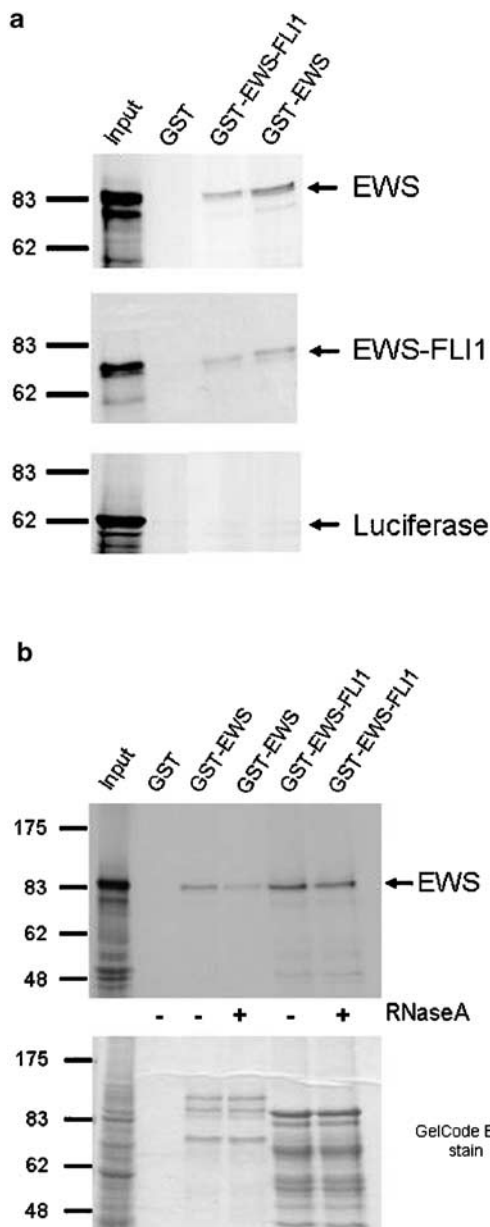


Figure 3 Confirmation of homo- and heterotypic interactions of EWS and EWS-FLI1 by GST pull-down assays. GST fusion proteins were purified from bacteria and incubated with *in vitro* translated, ³⁵S-labeled proteins. (a) EWS and EWS-FLI1 bind to GST-EWS and GST-EWS-FLI1, but not to GST. The control protein luciferase does not bind to any of the GST-fusion proteins. (b) EWS protein was incubated with GST-EWS or GST-EWS-FLI1 in the presence or absence of RNaseA as indicated. The GelCode stained gel demonstrates equal loading of GST fusion proteins

FLI1 in EFT is the TGFβ receptor type II (TGFβRII) promoter that is suppressed by the chimeric transcription factor. EWS-FLI1 directly binds to a 29 bp element (PRE2) located at position +1/+29 within the TGFβRII promoter (Hahm *et al.*, 1999). The PRE2 element comprises two tandem putative ets-binding sequences on the noncoding strand. Since we found EWS-FLI1 capable of forming homo-oligomers, we asked whether EWS-FLI1 binds to PRE2 as a monomer

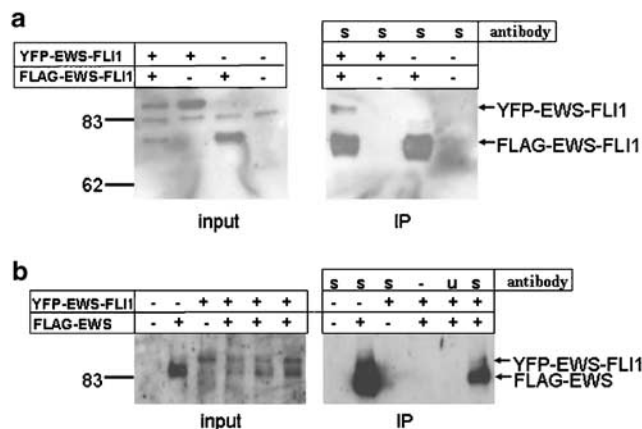


Figure 4 Coimmunoprecipitation of EWS-FLI1 with EWS-FLI1 and EWS. Cells were transfected with YFP-EWS-FLI1 and FLAG-EWS-FLI1 or FLAG-EWS, respectively. Immunoprecipitations were carried out with FLAG M2-antibody (s = specific) or CD99 antibody (u = unspecific), and blots were probed with antiserum 139-2, directed against the EWS N-terminus. (a) Specific precipitation of YFP-EWS-FLI1 with FLAG-EWS-FLI1, if both proteins were coexpressed. (b) Specific precipitation of FLAG-EWS with FLAG antibody and coprecipitation of YFP-EWS-FLI1 upon coexpression

or as a dimer. GAL4-EWS-FLI1 and EWS-FLI1 type 1 were *in vitro* transcribed and translated to obtain EWS-FLI1 proteins differing in size by 17 kDa. As shown in Figure 5a, translation of GAL4-EWS-FLI1 resulted in two protein products larger than untagged EWS-FLI1, one of the right size and one which was about 9 kDa smaller than expected, presumably due to the use of the first downstream methionine as initiation site. Similar quantities of *in vitro* translated proteins were used alone and in combination with each other in an electrophoretic mobility shift assay (EMSA) with a ³²P-labeled PRE2 probe (Figure 5b). Binding of EWS-FLI1 resulted in a single shifted band. Compatible with the presence of two differently sized proteins, GAL4-EWS-FLI1 binding generated two shifted bands. No intermediate products were observed, indicating binding of GAL4-EWS-FLI1 as a monomer rather than a dimer. This conclusion is further supported by the addition of EWS-FLI1 to GAL4-EWS-FLI1. Again, no other bands than the ones obtained with the individual proteins were observed. All band shifts were considered specific, since they disappeared upon the addition of cold specific, but not of unspecific, competitor, and they were supershifted by the addition of an antibody to the EWS N-terminus, but not to the EWS C-terminus that is absent from EWS-FLI1 fusion protein. These results confirm earlier observations (Hahm *et al.*, 1999; Lin *et al.*, 1999) that EWS-FLI1 binds to DNA as a monomer, even in the presence of two closely spaced ets-binding sites.

Discussion

In this study, we demonstrate for the first time, homotypic associations of the EFT-associated transcrip-

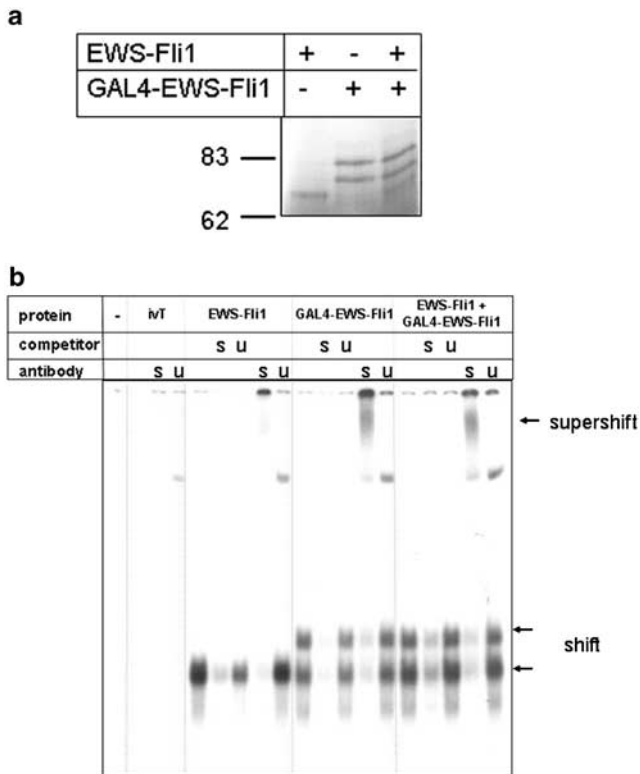


Figure 5 EWS-FLI1 binds to DNA as a monomer. **(a)** *In vitro* translation products: EWS-FLI1 and GAL4-EWS-FLI1 were transcribed and translated either separately (lanes 1 and 2) or together (lane 3). GAL4-EWS-FLI1 gave two products presumably due to the usage of alternative start codons. **(b)** EMSA showing DNA binding of EWS-FLI1 to the PRE2 probe of the TGF β RII promoter. Incubation of EWS-FLI1 with the probe resulted in one shifted band, incubation of GAL4-EWS-FLI1 resulted in two shifted complexes, compatible with the presence of two *in vitro* translated proteins that separately bind to DNA. When EWS-FLI1 and GAL4-EWS-FLI1 were cotranslated, no additional EMSA bands were observed, indicating the absence of mixed complexes between the proteins. The shifted complexes can be competed for by cold specific (s), but not unspecific (u) probe. In addition, the complexes could be supershifted with specific (s) antibody directed against the EWS N-terminus, but not with unspecific (u) antibody directed against the C-terminus of EWS

tion factor EWS-FLI1 and of its germline counterpart EWS, as well as weak interaction between the two proteins. These conclusions were primarily based on findings in *in vivo* protein interaction assays (FRET and two-hybrid driven reporter gene assays). *In vitro* physical interaction tests (GST-pull-down assays and coimmunoprecipitations) mostly confirmed these results. In the function-based interaction assays, results were highly dependent on the specific tag attached to the test proteins. It is likely that fusion to different protein tags differently affect the functional domains (protein interaction, DNA-binding or transactivation domains) due to structural constraints. Domain mapping experiments indicated that homo-oligomerization of EWS is dependent on the overall protein structure of the full-length protein, since all truncation constructs tested showed impaired interaction potential. However, the N-terminus of EWS was found to be sufficient for self-

association in the FRET experiments, while the cd in the context of either the N- or the C-terminus was required for cooperation in the reporter gene assays. In contrast, homotypic interaction of EWS-FLI1 was mediated primarily via the FLI1 C-terminus despite retention of the EWS N-terminus. In fact, the isolated FLI1 C-terminus efficiently interacted with full-length EWS-FLI1 and also with VP16-coupled germline FLI1, while no evidence for homotypic aggregation could be obtained for full-length FLI1. Thus it appears that homo-oligomerization between EWS-FLI1 molecules represents a gain of function, presumably due to altered protein conformation or accessibility of the FLI1 and EWS domains in the context of their oncogenic fusion. This interpretation may be supported by previous studies providing indirect evidence for conformational differences in the structure, accessibility and functionality of the EWS N-terminus between germline EWS and EWS-FLI1 and for a structural role of the FLI1 C-terminus in the transcriptional activity of EWS-FLI1. HsRBP7 was found to bind selectively to EWS-FLI1 and C-terminally truncated EWS but not to full-length EWS (Bertolotti *et al.*, 1998; Petermann *et al.*, 1998). Deletion of the FLI1 C-terminus was found to differently affect EWS-FLI1 driven transcriptional activation and repression (Arvand *et al.*, 2001), and retention of the EWS C-terminus blocked the transactivation activity of the EWS N-terminus (Li and Lee, 2000).

Our results, with respect to a possible heterotypic interaction between EWS and EWS-FLI1, were somehow ambiguous. Using FRET microscopy, we obtained only very few cells which were positive for interaction between YFP-EWS and CFP-EWS-FLI1 (data not shown). In the MTH system, the interaction between EWS-FLI1 and EWS was weak despite comparable protein expression levels. However, *in vitro* GST pull-down experiments confirmed the potential of EWS-FLI1 to form oligomers with EWS, but in line with the MTH results, the homotypic interactions were stronger than the observed heterotypic associations. The interaction of EWS-FLI1 with EWS in EFT cells would be of high interest if this would affect the normal function of the germline protein. We recently reported on an EFT in which the expression of EWS was completely lost and speculated whether loss of EWS function might be a general phenomenon in EFT (Kovar *et al.*, 2001). Since we did not detect any mutations that may impair EWS function in EWS expressing EFT, the interaction of EWS-FLI1 with EWS, if it actually exists, might be considered as an alternative mechanism of EWS inactivation through a dominant-negative competition. However, EWS is generally expressed at much higher levels than EWS-FLI1 and the weak associations observed are unlikely to allow for a functional impairment of the bulk of EWS in EFT cells. Conversely, the complete lack of EWS in the previously reported EFT indicates that EWS is not required for EWS-FLI1 function. Thus, there is no evidence so far to suggest that heterotypic interactions between EWS and EWS-FLI1 are important for EFT pathogenesis.

Several transcription factors are known to bind to DNA as a dimer. Therefore, it would not be unusual if the same would be true for EWS-FLI1. However, most ets proteins, including FLI1, normally recognize DNA in monomeric form (Carrere *et al.*, 1998b; Li and Lee, 2000). Accordingly, all published EMSA results for EWS-FLI1 demonstrated a single DNA-binding complex using *in vitro* translated protein (Hahm *et al.*, 1999; Lin *et al.*, 1999). In order to decide whether this complex contains EWS-FLI1 in monomeric or oligomeric form, we performed EMSAs of the TGF β R2 promoter PRE2 element (Hahm *et al.*, 1999) using mixtures of differently tagged and sized EWS-FLI1 proteins. However, we were unable to obtain hybrid complexes containing both EWS-FLI1 constructs. However, the TGF β R2 gene is transcriptionally repressed by EWS-FLI1. Thus, it cannot be excluded that certain activated genes may behave differently. Multimerization may be of particular importance to allow for binding of EWS-FLI1 to low-affinity ets-binding sites not recognized by germline FLI1, thus expanding the spectrum of target genes. In addition to its transcriptional activity, EWS-FLI1 has been demonstrated to exert a DNA-binding independent function in transformation (Jaishankar *et al.*, 1999; Welford *et al.*, 2001). It may be possible that EWS-FLI1 oligomerization or possibly heterodimerization with EWS is involved in this so far enigmatic activity of the oncogenic fusion protein.

Alternatively, oligomerization of EWS-FLI1 via the FLI1 domain may prevent DNA binding of EWS-FLI1. Homodimerization of EWS-FLI1 is reminiscent of EWS-WT1 in desmoplastic small round cell tumors (Ladanyi and Gerald, 1994). EWS-WT1 dimerizes via its fusion region, requiring both EWS and WT1 domains (Kim *et al.*, 1999). Interestingly, EWS-WT1 dimerization is blocked by phosphorylation, a prerequisite for DNA binding of monomeric EWS-WT1. It is tempting to speculate that a similar mechanism may regulate the DNA-binding activity of EWS-FLI1. While several kinases have already been shown to interact with EWS and evidence has been obtained for tyrosine and serine phosphorylations of the germline protein (Deloulme *et al.*, 1997; Guinamard *et al.*, 1997; Felsch *et al.*, 1999; Kim *et al.*, 2000; Olsen and Hinrichs, 2001), data on post-translational modifications of EWS-FLI1 are scarce. However, phosphorylation at serine 266 (encoded by EWS exon 8) has been found to regulate the transcriptional activity and the cellular compartmentalization of some EWS-FLI1 fusion types as well as of EWS-ATF1 of clear cell sarcoma, if EWS exon 8 is retained in the fusion (Olsen and Hinrichs, 2001).

In about 10% of EFT, the FLI1-DNA-binding component of the fusion protein is replaced by that of the closely related ERG protein (Sorensen *et al.*, 1994). ERG shows 81% homology to FLI1 on the amino acid level and, clinically, no differences between EFT with EWS-FLI1 and EWS-ERG fusions are evident (Ginsberg *et al.*, 1999). Thus, it is assumed that EWS-FLI1 and EWS-ERG function through the same mechanisms. Interestingly, ERG has been shown to form homodimers and to be able to heterodimerize with FLI1

(Carrere *et al.*, 1998a). Which domain is involved in the interaction of ERG with FLI1 has not been investigated so far. Domain mapping revealed that not only the N-terminal pointed domain of ERG, which is 82% identical to the pointed domain of FLI1 on the amino acid level, but also the ets-DNA-binding domain of ERG are needed for homodimerization. Thus, although the pointed domain is missing from EWS-ERG and EWS-FLI1 fusion proteins, it may be possible that EWS-ERG, like EWS-FLI1, is able to self-associate. The finding, that the ets-DNA-binding domain exhibits protein-protein interaction functions (Fitzsimmons *et al.*, 1996), supports our observations of association of full-length FLI1 and also EWS-FLI1 with CTD^{FLI1}. In fact, the self-association of EWS-FLI1 seems to be substantially mediated by the FLI1 domain. However, the possible association between FLI1 and EWS-FLI1 via their common C-terminus remains a theoretical possibility, as all EFT tested so far lack detectable expression of FLI1 (Kovar *et al.*, 1996). The role of self-association in EWS function awaits further investigation. Based on its relationship to the splicing factor TLS and the TFIID-associated protein TAFII68, as well as protein interactions with components of the basal transcriptional machinery (Bertolotti *et al.*, 1998) and the splicing apparatus (Zhang *et al.*, 1998; Knoop and Baker, 2000; Yang *et al.*, 2000), it is commonly assumed that EWS serves as a bridge between these two constituents of general gene expression. EWS is an RNA-binding protein and RNaseA sensitivity of GST pull-down reactions for EWS as well as the requirement for the presence of at least the partial RNA-binding domain in the MTH assay suggest a role for RNA binding in EWS homo-oligomerization. For EWS-FLI1 homotypic and heterotypic associations, binding to RNA is unlikely since the putative RNA-binding motifs present in the EWS central and CTDs are missing from the hybrid protein and RNaseA treatment did not affect its association with EWS in the GST pull down. Future studies will have to investigate the regulation and functional consequences of homotypic and heterotypic associations of EWS and its oncogenic transcription factor fusions.

Materials and methods

Cell culture and transfection

Human cell lines HeLa (ATCC CCL2) and SJ-NB7 (kindly provided by T Look, St Jude Children's Research Hospital, Memphis, USA) were grown in RPMI 1640 medium, supplemented with 10% fetal calf serum and penicillin/streptomycin. Transfections were carried out with Lipofectamine Plus reagent (Invitrogen, Groningen, The Netherlands), according to the manufacturer's instructions.

Plasmids

Constructs for FRET microscopy were as follows: full-length coding sequences of EWS-FLI1 type 1 and EWS were PCR amplified with primers containing suitable restriction sites. The PCR fragments were digested with *XhoI*-*HindIII* and ligated

into the pECFP-C1 and pEYFP-C1 vectors (Clontech Laboratories, Palo Alto, USA). The plasmids pECFP-EWS and pEYFP-EWS were digested with *Bam*HI, deleting 1.235 bp from the EWS C-terminus to generate constructs pECFP-NTD^{EWS} and pEYFP-NTD^{EWS}, coding for amino acids 1–245 of EWS. Constructs pECFP-CTD^{FLI1} and pEYFP-CTD^{FLI1} encoding amino acids 221–454 of human FLI1 were generated by cloning of the respective coding region into the pECFP-C1 and pEYFP-C1 vectors.

Constructs for the MTH system were as follows: the CheckMate MTH system (Promega, Madison, USA) was used for interaction analysis in mammalian cells, and the cloning was carried out in the provided vectors: pACT, containing the VP16 transactivation domain and pBIND, containing the GAL4-DNA-binding domain. The full-length coding region of EWS was amplified by PCR, using primers with suitable restriction sites to allow cloning into the MTH vectors. The full-length coding region of EWS-FLI1 type 1 was isolated by digestion of the vector pGEX-EWS-FLI1 (Spahn *et al.*, 2002) and ligated into the pACT and pBIND vectors, respectively. For the construct VP16-NTD^{EWS}, the cDNA encoding the N-terminus of EWS (amino acids 1–265) was generated by PCR, and ligated into the pACT vector. The construct GAL4-NTD^{EWS} was described elsewhere (Petermann *et al.*, 1998). The EWS deletion constructs cd^{EWS} (amino acids 151–472), Ncd^{EWS} (amino acids 1–472), cdC^{EWS} (amino acids 151–656) and CTD^{EWS} (amino acids 265–656) were generated by PCR and cloned into pBIND and pACT vectors. cDNAs encoding full-length FLI1 or the C-terminus of FLI1 (CTD^{FLI1}, amino acids 219–452) were PCR amplified and ligated into the pACT and pBIND vectors. For all constructs, integrity of the entire coding sequences and expression of proteins were confirmed by sequencing and Western blot analysis, respectively.

GST fusion constructs were as follows: the full-length coding regions of EWS-FLI1 type 1 and EWS were PCR amplified and cloned in frame with the glutathione S-transferase (GST) gene of *Schistosoma japonicum* into pGEX-5X-1 vector (Amersham Biosciences, Uppsala, Sweden).

FLAG-tagged constructs for immunoprecipitation reactions have been described elsewhere (Spahn *et al.*, 2002).

FRET microscopy

HeLa or SJ-NB7 cells were seeded on fibronectin-coated round glass cover slips and transfected with the indicated pECFP-C1 and pEYFP-C1 expression vectors. At 24 or 48 h after transfection, cells were fixed with 2% formaldehyde at room temperature for 15 min and covered with PBS. For FRET microscopy, the cover slips were transferred into a suitable chamber, covered with PBS and analysed with a Nikon Diaphot TMD microscope. Images of YFP and CFP fluorescence were taken with appropriate filter sets (Omega optical Inc., Brattleboro, USA; YFP filter set: excitation 500 nm, dichroic mirror 525 nm, emission 535 nm; CFP filter set: excitation 440 nm, dichroic mirror 455 nm, emission 480 nm; FRET filter set: excitation 440 nm, dichroic mirror 455 nm, emission 535 nm) and with a cooled charge-coupled device camera (Kappa GmbH, Gleichen, Germany). For acceptor photobleaching FRET microscopy, as reviewed in Schmid and Sitté (2003), cells were imaged with an oil immersion objective and images were captured with the donor filter using a 90% neutral density filter to prevent donor bleaching. This was followed by bleaching of the FRET acceptor (EYFP) with the appropriate filter set in the absence of the neutral density filter using a 100 W Mercury lamp for about 45–60 s. Subsequently, the neutral filter was again placed

in the excitation light path and another image was taken with the ECFP-filter set under the same camera setting as the first one. An increase in the donor-fluorescence intensity was visualized by calculating a ratio image of the ECFP-image before and after acceptor photobleaching using NIH-Image software or the WindowsTM-equivalent ScionImage (Scion Corporation Inc., MD, USA). The three-filter method (Xia and Liu, 2001) was used to analyse the interactions of FLI1, CTD^{FLI1} and NTD^{EWS}. YFP, CFP and FRET filter images were taken with the same camera and microscope settings. The FRET filter image contains the FRET signal, and also the bleed-through of YFP and CFP into the FRET channel. Cells transfected with YFP or CFP only were used to determine the correction factors for bleed-through of YFP ($a=0.52$) and CFP fluorescence ($b=0.54$). The YFP and CFP images of the samples were then multiplied with the respective correction factor and subtracted from the FRET image, resulting in FRET_N. The FRET_N image represents the fluorescence due to FRET only. All image calculations were carried out with the NIH image software version 1.62.

MTH system

SJ-NB7 cells were seeded into 24-well plates and transfected with the indicated pACT and pBIND expression vectors and the pG5luc reporter vector, provided by the CheckMate MTH system kit (Promega, Madison, USA). Transfections were carried out on average five times in quadruplicates, three times for luciferase assay measurements and one time in cotransfection with pEGFP-CMV for determination of transfection efficiency by FACS (FACS Calibur, Becton Dickinson, Sunnyvale, CA, USA). Luciferase expression was measured with the BrightGlo Luciferase Assay System (Promega, Madison, USA) 24 h after transfection, according to the manufacturer's instructions. Values were corrected for transfection efficiency.

GST pull-down experiments

Vectors pGEX-5X-1, pGEX-EWS and pGEX-EWS-FLI1 type 1 were transformed into *E. coli* XL1blueMRF⁻. The expression of GST-only protein was induced by 1 mM IPTG for 2 h at 37°C, of GST-EWS by 0.1 mM IPTG for 2 h at 25°C and of GST-EWS-FLI1 by 0.1 mM IPTG for 5 h at 25°C. The soluble protein fraction was purified by affinity binding to Glutathione Sepharose 4B beads (Amersham Biosciences, Uppsala, Sweden). For the pull-down experiments, approximately 2 μg of GST-fusion protein coated beads were incubated for 2 h in Kleiman buffer (150 mM NaCl, 3 mM KCl, 10 mM Na₂HPO₄, 1.8 mM KH₂PO₄, 0.01% NP-40, 0.04% BSA and 'complete' protease inhibitor cocktail (Roche Diagnostics, Mannheim, Germany) (Kleiman and Manley, 1999)) with ³⁵S-labeled EWS, EWS-FLI1 type 1 or luciferase proteins, generated with the TNT T7Quick Coupled Transcription/Translation System (Promega, Madison, USA). After washing with Kleiman buffer containing 300 mM NaCl three times, protein complexes were resolved on an 8.5% SDS-PAGE and analysed by autoradiography. Where indicated, incubations of GST-coupled proteins with *in vitro* translated proteins was performed in the presence of 10 μg RNaseA.

Immunoprecipitations

For coimmunoprecipitations, SJ-NB7 cells expressing FLAG- and YFP-tagged proteins were harvested 48 h after transfection and lysed in HUNT-buffer (100 mM NaCl, 20 mM Tris-HCl pH 8.0, 1 mM EDTA, 0.5% NP-40, Complete Protease Inhibitor Cocktail (Roche Diagnostics, Mannheim,

Germany)). Protein extracts were added to Dynabeads M-450 (DynaL, Oslo, Norway), precoupled with anti-FLAG M2 antibody (Sigma, St Louis, USA) and incubated for 2 h at 4°C. After washing with HUNT-buffer, protein complexes were resolved on 8.5% SDS-PAGE. Western blots were probed with EWS antiserum 139-2, raised against the N-terminus of EWS (amino acids 1–82; kindly provided by CT Denny, UCLA).

Electrophoretic mobility shift assays

For DNA-binding studies of EWS-FLI1 type 1, the 29 bp TGF β R2 promoter PRE2 probe (Hahm *et al.*, 1999) was end labeled by T4 polynucleotide kinase (New England Biolabs, Beverly, USA) with γ -³²P-ATP (Hartmann Analytic, Braunschweig, Germany) and used as a probe. EWS-FLI1 type 1 and GAL4-EWS-FLI1 type 1 were generated using the TNT T7 Quick Coupled Transcription/Translation kit (Promega, Madison, USA) and the vectors pBS STA7 (containing the full-length coding region of EWS-FLI1 type 1, provided by O Delattre, Institut Curie, Paris, France) and pBIND-EWS-FLI1 type 1 (see above) as templates. To control for efficient *in vitro* translation, parallel reactions were carried out in the presence

of ³⁵S-labeled methionine/cysteine and proteins were analysed by SDS-PAGE and autoradiography. Where indicated, 3 μ l of cold *in vitro* translated protein were preincubated with either cold specific or nonspecific competitor probe or antibodies in 2 \times binding buffer (40 mM Hepes, pH 7.9, 2 mM MgCl₂, 10% glycerol, 80 mM KCl, 200 μ M EDTA, 0.2% NP-40, 1 μ g poly(dIdC)–poly(dIdC)) for 10 min at room temperature, then 2 \times 10⁴ cpm of labeled probe was added. After incubation for 15 min at room temperature, complexes were resolved on a 5% polyacrylamide gel in 0.5 \times TBE and the dried gel was exposed to X-ray film. Nonlabeled PRE2 probe and the PCR fragment of the FLI1 C-terminus (702 bp) were used as specific and nonspecific competitor sequences, respectively. For the super-shift experiments, 138-2 (raised against the N-terminus of EWS; provided by CT Denny, UCLA, USA) and SE680 (raised against the C-terminus of EWS; provided by O Delattre, Institut Curie, Paris, France) were used as specific and nonspecific antibodies, respectively.

Acknowledgements

This study was supported in part by Grants 13708GEN and 14299GEN of the Austrian Science Fund.

References

- Arvand A, Bastians H, Welford SM, Thompson AD, Ruderman JV and Denny CT. (1998). *Oncogene*, **17**, 2039–2045.
- Arvand A, Welford SM, Teitell MA and Denny CT. (2001). *Cancer Res.*, **61**, 5311–5317.
- Bailly RA, Bosselut R, Zucman J, Cormier F, Delattre O, Roussel M, Thomas G and Ghysdael J. (1994). *Mol. Cell. Biol.*, **14**, 3230–3241.
- Bertolotti A, Melot T, Acker J, Vigneron M, Delattre O and Tora L. (1998). *Mol. Cell. Biol.*, **18**, 1489–1497.
- Carrere S, Verger A, Flourens A, Stehelin D and Dutertre-Coquillaud M. (1998a). *Oncogene*, **16**, 3261–3268.
- Carrere S, Verger A, Flourens A, Stehelin D and Dutertre-Coquillaud M. (1998b). *Oncogene*, **16**, 3261–3268.
- Chansky HA, Hu M, Hickstein DD and Yang L. (2001). *Cancer Res.*, **61**, 3586–3590.
- Dauphinot L, De Oliveira C, Melot T, Sevenet N, Thomas V, Weissman BE and Delattre O. (2001). *Oncogene*, **20**, 3258–3265.
- Delattre O, Zucman J, Plougastel B, Desmaze C, Melot T, Peter M, Kovar H, Joubert I, De Jong P and Rouleau G. *et al.* (1992). *Nature*, **359**, 162–165.
- Deloulme JC, Prichard L, Delattre O and Storm DR. (1997). *J. Biol. Chem.*, **272**, 27369–27377.
- Felsch JS, Lane WS and Peralta EG. (1999). *Curr. Biol.*, **9**, 485–488.
- Feng L and Lee KA. (2001). *Oncogene*, **20**, 4161–4168.
- Fitzsimmons D, Hodsdon W, Wheat W, Maira SM, Wasyluk B and Hagman J. (1996). *Genes Dev.*, **10**, 2198–2211.
- Fukuma M, Okita H, Hata J and Umezawa A. (2003). *Oncogene*, **22**, 1–9.
- Ginsberg JP, De Alava E, Ladanyi M, Wexler LH, Kovar H, Paulussen M, Zoubek A, Dockhorn-Dworniczak B, Juergens H, Wunder JS, Andrusik IL, Malik R, Sorensen PH, Womer RB and Barr FG. (1999). *J. Clin. Oncol.*, **17**, 1809–180.
- Guinamard R, Fougereau M and Seckinger P. (1997). *Scand. J. Immunol.*, **45**, 587–595.
- Hahm KB, Cho K, Lee C, Im YH, Chang J, Choi SG, Sorensen PH, Thiele CJ and Kim SJ. (1999). *Nat. Genet.*, **23**, 222–227.
- Jaishankar S, Zhang J, Roussel MF and Baker SJ. (1999). *Oncogene*, **18**, 5592–5597.
- Kim J, Lee JM, Branton PE and Pelletier J. (1999). *Proc. Natl. Acad. Sci. USA*, **96**, 14300–14305.
- Kim J, Lee JM, Branton PE and Pelletier J. (2000). *FEBS Lett.*, **474**, 121–128.
- Kleiman FE and Manley JL. (1999). *Science*, **285**, 1576–1579.
- Kleiman FE and Manley JL. (2001). *Cell*, **104**, 743–753.
- Knoop LL and Baker SJ. (2000). *J. Biol. Chem.*, **275**, 24865–24871.
- Knoop LL and Baker SJ. (2001). *J. Biol. Chem.*, **276**, 22317–22322.
- Kovar H, Aryee DN, Jug G, Henockl C, Schemper M, Delattre O, Thomas G and Gadner H. (1996). *Cell Growth Differ.*, **7**, 429–437.
- Kovar H, Jug G, Hattinger C, Spahn L, Aryee DN, Ambros PF, Zoubek A and Gadner H. (2001). *Cancer Res.*, **61**, 5992–5997.
- Ladanyi M and Gerald W. (1994). *Cancer Res.*, **54**, 2837–2840.
- Lessnick SL, Braun BS, Denny CT and May WA. (1995). *Oncogene*, **10**, 423–431.
- Lessnick SL, Dacwag CS and Golub TR. (2002). *Cancer Cell*, **1**, 393–401.
- Li KK and Lee KA. (2000). *J. Biol. Chem.*, **275**, 23053–23058.
- Li R, Pei H and Watson DK. (2000). *Oncogene*, **19**, 6514–6523.
- Lin PP, Brody RI, Hamelin AC, Bradner JE, Healey JH and Ladanyi M. (1999). *Cancer Res.*, **59**, 1428–1432.
- Matsumoto Y, Tanaka K, Nakatani F, Matsunobu T, Matsuda S and Iwamoto Y. (2001). *Br. J. Cancer*, **84**, 768–775.
- Mavrothalassitis G and Ghysdael J. (2000). *Oncogene*, **19**, 6524–6532.
- May WA, Arvand A, Thompson AD, Braun BS, Wright M and Denny CT. (1997). *Nat. Genet.*, **17**, 495–497.
- May WA, Gishizky ML, Lessnick SL, Lunsford LB, Lewis BC, Delattre O, Zucman J, Thomas G and Denny CT. (1993). *Proc. Natl. Acad. Sci. USA*, **90**, 5752–5756.
- Ohno T, Rao VN and Reddy ES. (1993). *Cancer Res.*, **53**, 5859–5863.
- Olsen RJ and Hinrichs SH. (2001). *Oncogene*, **20**, 1756–1764.

- Ouchida M, Ohno T, Fujimura Y, Rao VN and Reddy ES. (1995). *Oncogene*, **11**, 1049–1054.
- Petermann R, Mossier BM, Aryee DN, Khazak V, Golemis EA and Kovar H. (1998). *Oncogene*, **17**, 603–610.
- Rao VN, Ohno T, Prasad DD, Bhattacharya G and Reddy ES. (1993). *Oncogene*, **8**, 2167–2173.
- Schmid JA, Scholze P, Kudlacek O, Freissmuth M, Singer EA and Sitte HH. (2001). *J. Biol. Chem.*, **276**, 3805–3810.
- Schmid JA and Sitte HH. (2003). *Curr. Opin. Oncol.*, **15**, 55–64.
- Sorensen PH, Lessnick SL, Lopez Terrada D, Liu XF, Triche TJ and Denny CT. (1994). *Nat. Genet.*, **6**, 146–151.
- Spahn L, Petermann R, Siligan C, Schmid JA, Aryee DN and Kovar H. (2002). *Cancer Res.*, **62**, 4583–4587.
- Thompson AD, Braun BS, Arvand A, Stewart SD, May WA, Chen E, Korenberg J and Denny C. (1996). *Oncogene*, **13**, 2649–2658.
- Toretsky JA, Connell Y, Neckers L and Bhat NK. (1997). *J. Neurooncol.*, **31**, 9–16.
- Venkitaraman AR. (2001). *J. Cell Sci.*, **114**, 3591–3598.
- Welford SM, Hebert SP, Deneen B, Arvand A and Denny CT. (2001). *J. Biol. Chem.*, **276**, 41977–41984.
- Xia Z and Liu Y. (2001). *Biophys. J.*, **81**, 2395–2402.
- Yang L, Chansky HA and Hickstein DD. (2000). *J. Biol. Chem.*, **275**, 37612–37618.
- Zhang D, Paley AJ and Childs G. (1998). *J. Biol. Chem.*, **273**, 18086–18091.
- Zwerner JP and May WA. (2001). *Oncogene*, **20**, 626–633.